GHOST SV Observation Evaluation Form

Title: **Characterization of a solar-type star WASP-108 and its transiting hot Jupiter**

Program ID: GS-2023A-SV-102

Authors: Eder Martioli & Diego Lorenzo de Oliveira

Description of the primary goals and the main findings

In summary, the primary goals of these observations are the following:

1. Detecting the atmosphere of the exoplanet WASP-108b from transmission spectroscopy;

2. Detecting the Rossiter-McLaughlin effect and measure the spin-orbit alignment of the system;

3. Measure stellar parameters and elemental abundances of the solar twin 18 Sco and use it as reference to obtain improved parameters of WASP-108.

Main findings:

1. **Detecting the atmosphere of the exoplanet WASP-108b from transmission spectroscopy**

As an ambitious test with this experiment, we attempted to perform differential photometry on each spectral bin of GHOST spectra taking advantage of the dual target mode, where the spectra of WASP-108 and a reference star are recorded simultaneously. We obtained continuous observations during 5 hours bracketing a transit of WASP-108b. The expected transit depth of WASP-108b is about 1.3%. The preliminary results are illustrated in Figure 1. The time series of the magnitude difference between the two targets is strongly affected by systematics, showing that the relative throughput between the two IFUs is unstable. Therefore, the transit of WASP-108b cannot be detected by this method, unless a more careful analysis of these data allows the systematics to be calibrated, which will be explored in the paper in preparation.

The possible reasons for this instability between the IFUs may be due to the variable transmission of the fiber bundles, which are affected by several aspects, such as guiding, seeing variations, centering, etc. A possible improvement to mitigate these effects could be, for example, to use an independent set up of guiding for each IFU.

To conclude this part, as the transit of WASP-108 could not be detected, it is not possible to measure the transit depth as a function of wavelength, and therefore, it is not possible to detect the planet's atmospheric features by transmission spectroscopy. However, a more standard method to detect the atmosphere of WASP-108b can still be applied to these data, using cross-correlation between atmospheric models and the residual spectra, where the residual spectra is calculated by constructing an out-of-transit stellar template and dividing the spectrum by this template to remove the stellar contribution. This technique has not yet been applied to our data, but will also be explored in the paper in preparation.

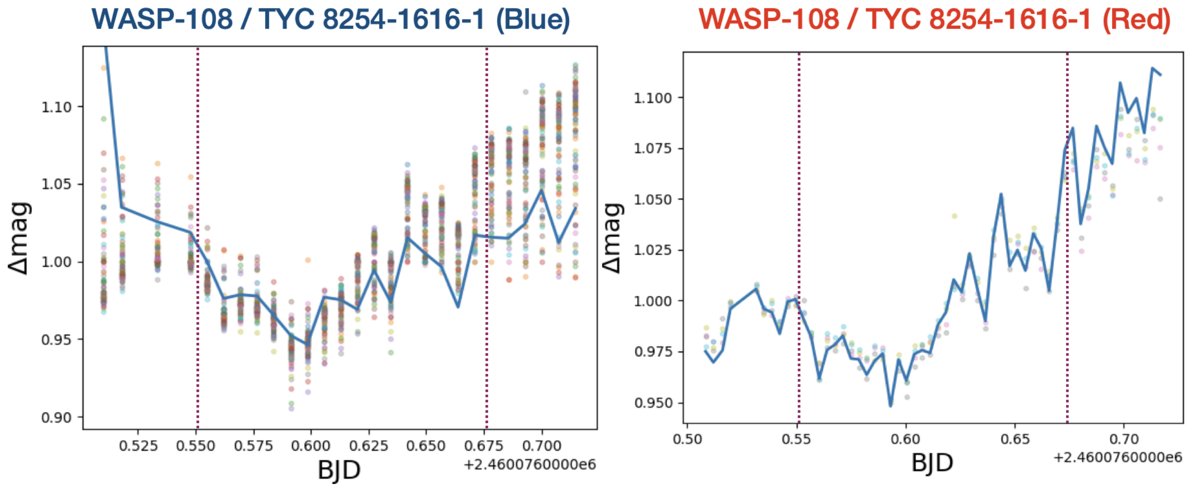

Figure 1 - Time series of the differential "photometry" between WASP-108 and the reference star TYC8254-1616-1 for the blue (left) and red (right) channels of GHOST. Each point shows the magnitude difference between the two targets in each 2-nm spectral bin of the GHOST spectrum. The vertical lines show the expected ingress and egress times of the transit of WASP-108b.

2. Rossiter-McLaughlin effect and the spin-orbit alignment of WASP-108

We analyzed the GHOST reduced spectra of WASP-108 (observed with IFU1) using the methods of Martioli et al. (2022), as illustrated in Figure 2. We have also analyzed the spectra of the reference star TY-8254-1616-1 (observed with IFU2) using exactly the same methods. We applied a cross correlation function (CCF) analysis between a weighted G2 mask and the GHOST spectra, where we obtained an extremely stable time series of CCFs during the 5 hours sequence, including the full transit of the hot-Jupiter WASP-108b. We obtained an rms dispersion for the residual CCFs of the order of 0.05%, as shown in Figure 3.

We measured radial velocities (RV) using a CCF template matching technique (Martioli et al., 2020, 2022) for both targets. The RVs of the reference star show a linear instrumental drift, which calibrates the main target RVs. We detected the transit of WASP-108b in the calibrated RV time series, as illustrated in Figure 4.

We modeled the Rossiter-McLaughlin effect to measure the spin-orbit alignment of the system from which we obtained an obliquity of λ=6.6°±1.1°. The final rms dispersion of the WASP-108 RV residuals is 6.3 m/s in the blue channel and 9.2 m/s in the red channel. Figure 5 shows the Dopper tomography maps of WASP-108 and of the reference star TY-8254-1616-1, where the Doppler shadow of the planet WASP-108b during the transit can be clearly seen.

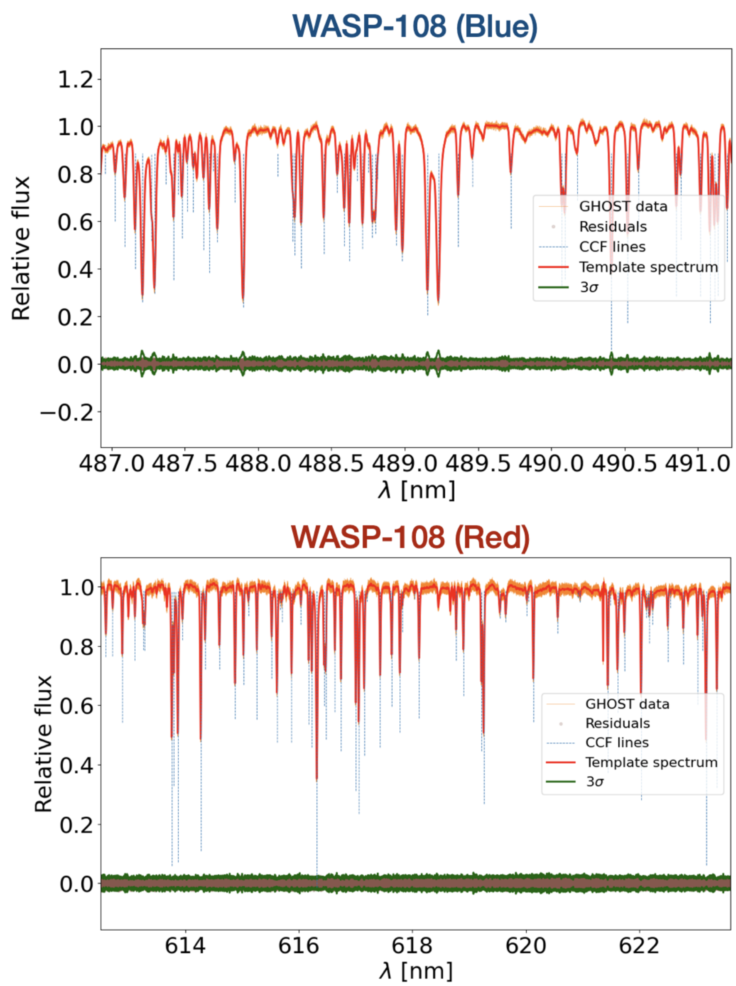

Figure 2 - GHOST spectra of WASP-108. The orange lines show all individual reduced spectra of WASP-108 obtained in the time series, the red lines show the median of all spectra, the vertical dashed blue lines show the lines in the CCF mask with their sizes proportional to their respective weights, the brown lines show the residuals and the green lines show the ±1-sigma of each spectral bin.

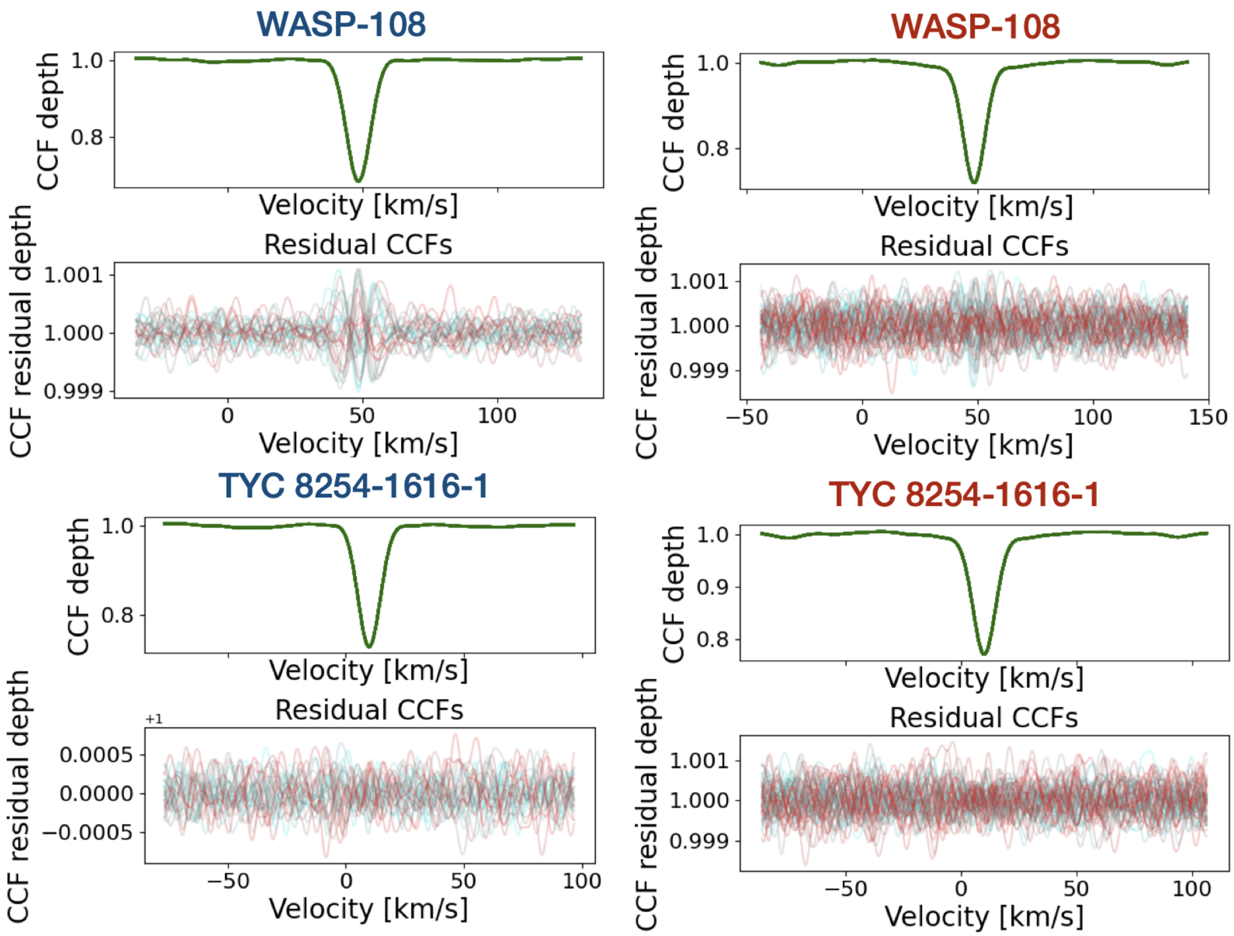

Figure 3 - CCF analysis of WASP-108 and TYC 824-1616-1 GHOST spectra. The left panels show the CCF results for the blue channel and the right panels show the CCF results for the red channel. The weighted mean CCFs obtained for each spectrum are displayed in the color code that shows the first epoch in dark blue and the last epoch in dark red. The green lines show the weighted mean of all CCF data, and the bottom panels show the CCF residuals after subtracting the mean CCF.

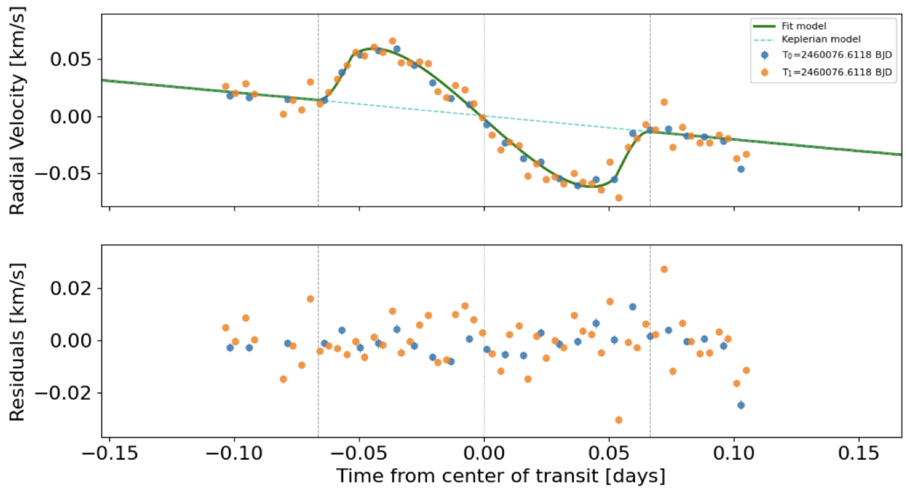

Figure 4 - Rossiter-McLaughlin effect on the transit of WASP-108b observed by GHOST. The blue points show the radial velocity data taken from the blue channel and the orange points show the data taken from the red channel. The green line shows the best-fit RV model, including the RM effect, and the dashed blue line shows the RV model of the Keplerian motion.

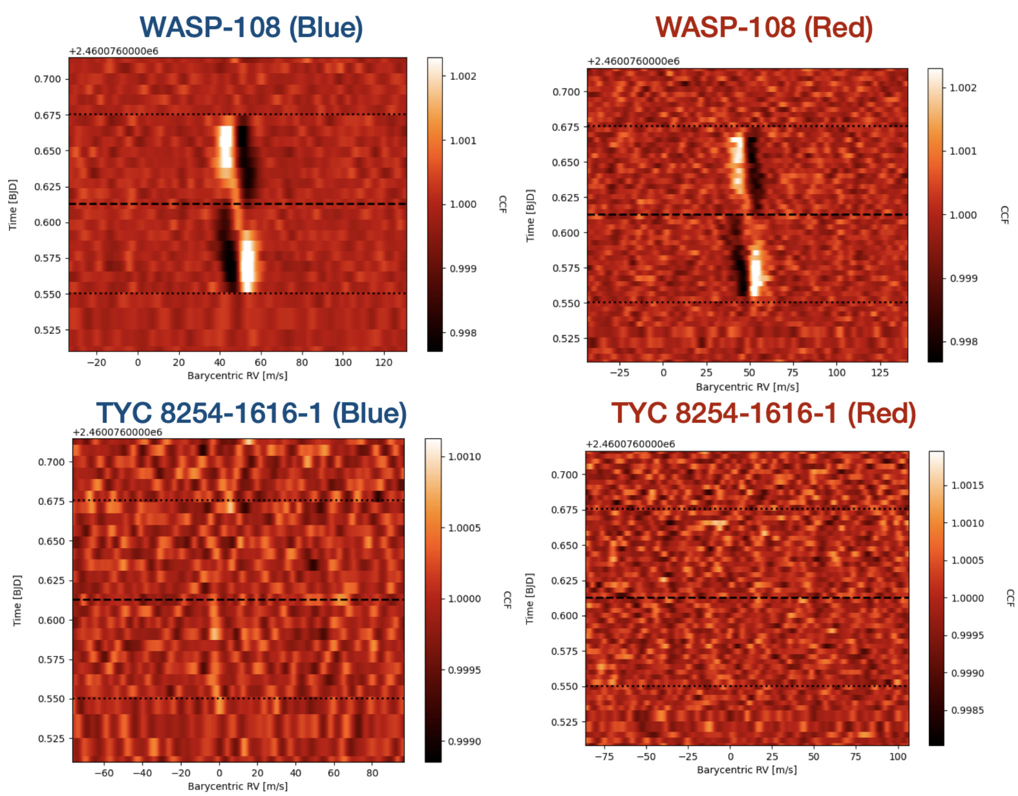

Figure 5 - Residual CCF data (CCF divided by the mean out-of-transit CCF) for WASP-108 and TYC 8254-1616-1 in both channels of GHOST. The horizontal black lines show the predicted time of ingress, the center of transit, and egress. The Doppler shadow signature of the planet WASP-108b is clearly detected during the transit, whereas the reference star is absent from any signal.

3. Stellar parameters of the solar twin 18 Sco, and a differential analysis of WASP-108

We observed the bright solar twin 18 Sco to confirm the capability of GHOST to determine the stellar parameters and abundances of solar-type stars. Figure 6 shows the high signal-to-noise spectrum of 18 Sco, from which we measured the stellar parameters, as follows.

Parameter	**SOPHIE data**	**Ghost data: Red channel**	**Ghost data: Red & Blue channels**	**Literature (diff. analysis)**	**Offsets (Literature - Ghost)**
Effective Temperature (K)	5723 ± 27 ±10	5730± 25 ±7	5718± 20 ±9	5817 ± 4	+99 ± 20 K ± 9K
Surface gravity (dex)	4.29 ± 0.07 ±0.005	4.273±0.06 ±0.001	4.249±0.05 ±0.005	4.448± 0.012	+0.199 ±0.05 ± 0.005
Metallicity [Fe/H]	+0.00 ± 0.02 ±0.01	+0.029±0.01 9 ±0.006	+0.02±0.02 ±0.008	+0.052±0.005	+0.03 ± 0.02 ±0.008
Turbulence velocity (km/s)	0.86 ± 0.05 ±0.015	0.870±0.069 ±0.020	0.87±0.04 ±0.02	1.02 ± 0.005 ± 0.04	+0.15 ± 0.04 ±0.04

Table 1 - Spectroscopic parameters estimated using GHOST and SOPHIE spectra of 18 Sco. We show the average results from Kurucz and MARCS atmospheric models. The reported errors come from the internal uncertainties of the spectroscopic equilibrium method and the systematic errors arise from comparison between the adopted model of atmospheres. The fifth column shows the literature's values of 18 Sco' high-precision parameters using strictly differential analysis (e.g. Bazot et al. 2018). The last column shows the differences between the estimates from the literature and the absolute atmospheric parameter estimates.

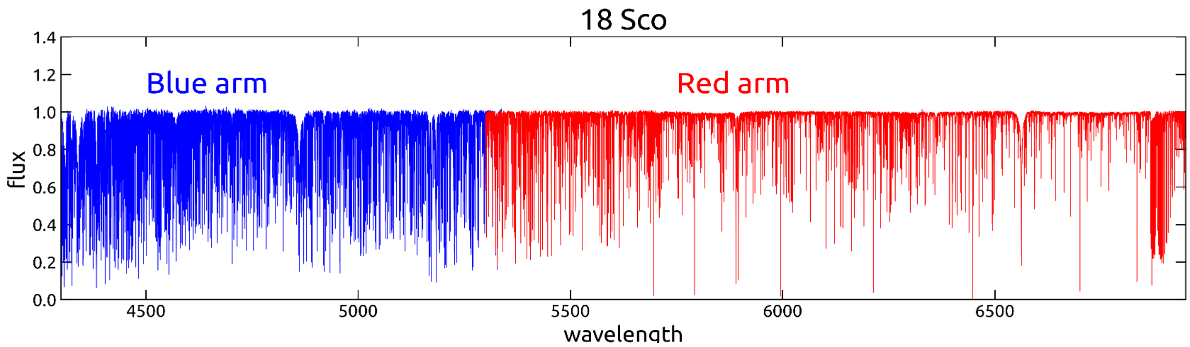

Figure 6 - GHOST spectrum of the solar twin 18 Sco. The blue line shows the average of 2 spectra of 18 Sco observed by the blue arm of GHOST with an exposure time of 120 s, and the red line shows the average of 8 spectra of 18 Sco observed by the red arm of GHOST with an exposure time of 30 s.

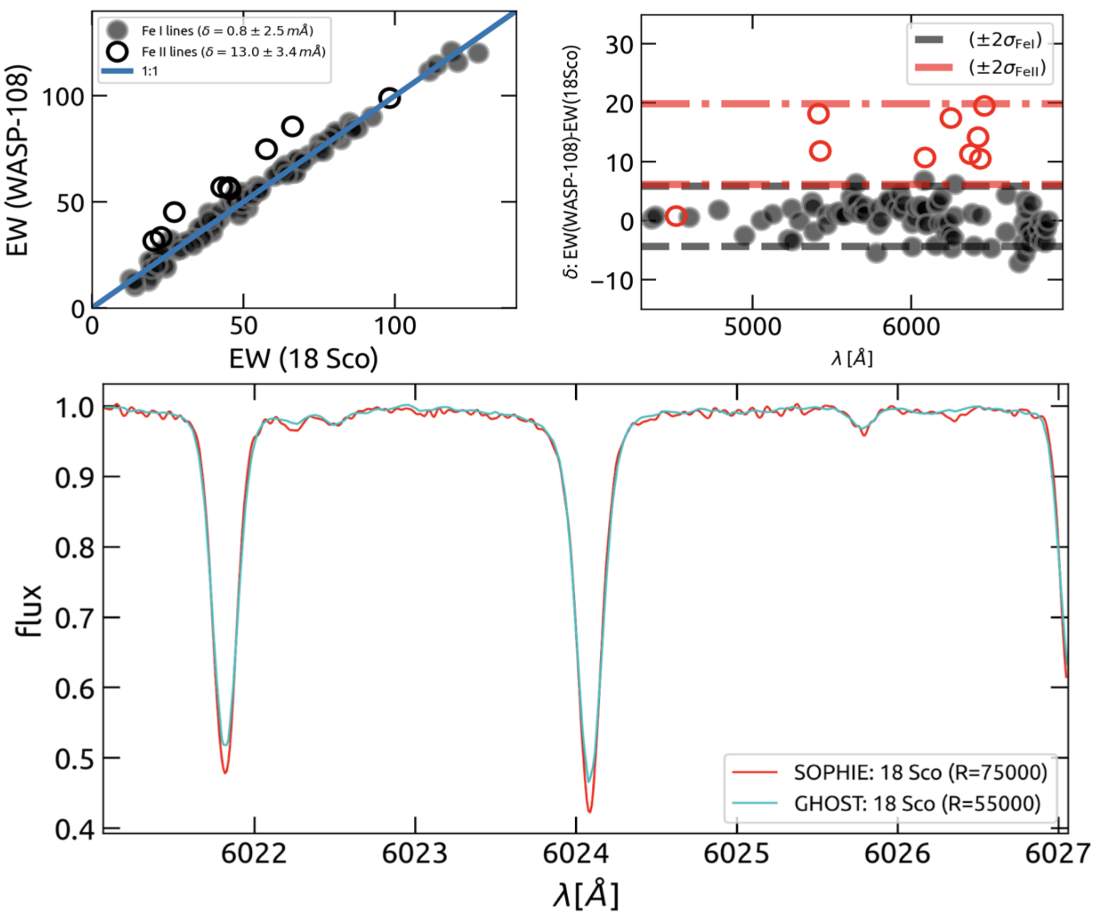

Figure 7 - Upper left panel: EW measurements for 18 Sco and WASP-108. Filled and empty circles are Fe I and Fe II EWs, respectively. Upper right panel: EW differences between WASP-108 and 18 Sco as a function of wavelength. Lower panel: Narrow spectral range bracketing the isolated Fe I line at 6024 angstroms. GHOST (cyan solid line) and SOPHIE (solid red line) spectra of the solar twin 18 Sco.

Ideally, one should use a solar spectrum obtained, for example, from observations of the reflected sunlight on the Moon or on asteroids, to use it as a reference to employ a strictly differential analysis for accurate determination of the spectroscopic parameters of stars that are similar to our Sun, as WASP-108. However, the ways to obtain a solar spectrum are not yet feasible with GHOST. Thus, we will use the solar twin 18 Sco as a reference to obtain the differential analysis of WASP-108, hoping to improve the parameters for this star, and, consequently, to improve the determination of the planetary parameters of its hot Jupiter WASP-108b.

We normalized in a self-consistent way the 18 Sco and WASP-108 spectra covering the λλ4300-6950 region. We measured EW of 75 Fe I and 9 Fe II lines from Meléndez et al. 2014 line list for both stars. Then, we derived their atmospheric parameters through the method of spectroscopic equilibrium of Fe I and Fe II lines (e.g. Yana Galarza et al. 2019). In Table 1, we show the absolute spectroscopic analysis using SOPHIE and GHOST data. We found similar offsets of ~100 K in relation to the 18 Sco' interferometric effective temperature (Teff = 5819±31 K, Karovicova et al. 2022) and high-precision differential parameters collected from the literature (see Table 1). The remaining atmospheric parameters show offsets of ~+0.2 dex, +0.02 dex, and 0.15 km/s for surface gravity, metallicity, and micro-turbulence. This feature highlights the importance of comparing the absolute spectroscopic parameters with other independent measurements. The results for WASP-108 are shown in Table 2.

Parameter	Absolute analysis	offsets	Absolute Analysis +offsets	Differential analysis	Parameter (Anderson et al. 2014)
Effective Temperature (K)	6048 ± 32 ± 8	+99 ± 20 K ± 9K	6147 ± 37 ± 9	6134 ± 16 ± 0.562	6000 ± 140
Surface gravity (dex)	4.22 ±0.06 ±0.00	+0.199 ±0.05 ± 0.005	4.424 ± 0.08 ±0.005	4.409 ± 0.042 ± 0.004	4.15 ± 0.20
Metallicity [Fe/H]	+0.178 ±0.025 ±0.006	+0.03 ± 0.02 ±0.008	+0.218 ± 0.03 ± 0.01	+0.210 ± 0.012 ± 0.004	+0.05 ± 0.1
Turbulence velocity (km/s)	1.17 ± 0.05 ± 0.01	+0.15 ± 0.04 ±0.04	1.32 ± 0.05 ±0.04	1.315 ± 0.033 ± 0.005	1.2 ± 0.1

Table 2 - Spectroscopic parameters estimated using GHOST and SOPHIE spectra of 18 Sco. We show the average results from Kurucz and MARCS atmospheric models. The reported errors come from the internal uncertainties of the spectroscopic equilibrium method and the systematic errors arise from comparison between the adopted model of atmospheres. The fifth column shows the 18 Sco' high-precision parameters using strictly differential analysis (e.g. Bazot et al. 2018). The last column is the difference between the estimates from the literature (fifth column) and the absolute atmospheric parameter estimates.

4. Conclusions

In this SV project, GHOST was used to obtain time series observations in dual target standard resolution mode to observe a transit of the hot Jupiter WASP-108b. In addition, we observed the bright solar twin 18 Sco, as a solar standard. These observations allowed us to test GHOST's ability to perform differential time series using simultaneous observations of a reference star. It also allowed us to investigate the spectroscopic stability of GHOST over a time series of a few hours, which turned out to be extremely stable, providing a superb measurement of the Rossiter-McLaughlin effect for WASP-108b. Finally, as expected, GHOST proved to be an excellent instrument for stellar characterization, where we applied both an absolute analysis and a strictly differential analysis to obtain the stellar parameters.

Additional comments on GHOST performance:

The data have been reduced using the SV version of the GHOST pipeline, where we turned off the sky subtraction and performed our own post-processing analysis starting with the *calibrated.fits products. The wavelength calibration performed by the pipeline is excellent and we had no issues with the extracted spectra, although our observations are of relatively high SNR.

The strongest feature noted in our observations was the high instrumental stability over a time series of 5 hours. This shows the potential of GHOST to perform high precision radial velocity work as well as for the detection of the atmosphere of exoplanets, which requires stability as well. In addition to the stability, GHOST has shown to produce a high quality and high signal-to-noise spectra in both channels, which makes it extremely competitive for several works on the determination of stellar parameters and abundances for ranges of magnitudes never achieved before.

Suggestions for improvements:

Enable observation of non-sidereal targets. In particular, for GHOST it is important to observe asteroids, as they provide a good reference solar spectrum to perform differential analyzes of Sun-like stars with greater accuracy for the determination of stellar parameters and abundances.